Weierstraß-Institut für Angewandte Analysis und Stochastik

im Forschungsverbund Berlin e.V.

Preprint ISSN 0946 – 8633

Cascaded self-compression of femtosecond pulses in filaments

Carsten Brée [1,2], Jens Bethge[2], Stefan Skupin[3,4], Luc Bergé[5], Ayhan Demircan[1], and Günter Steinmeyer[2,6]

submitted: 21. Jan. 2010

[1] Weierstrass Institute for Applied Analysis and Stochastics, Mohrenstraße 39, 10117 Berlin, Germany

[2] Max Born Institute for Nonlinear Optics and Short Pulse Spectroscopy, Max-Born-Straße 2A, 12489 Berlin, Germany

[3] Max-Planck-Institut für Physik komplexer Systeme, 01187 Dresden, Germany

[4] Institut für Festkörpertheorie und -optik, Friedrich-Schiller-Universität, 07743 Jena, Germany

[5] CEA-DAM, DIF, 91297 Arpajon, France

[6] Optoelectronics Research Centre, Tampere University of Technology, 33101 Tampere, Finland

No. 1478

Berlin 2010

2000 *Mathematics Subject Classification.* Primary 78A60, 81V80, 35Q55, 37K40 .

Key words and phrases. Nonlinear Schrödinger Equations, Optical self-focusing, Ultrashort pulse propagation.

We kindfully acknowledge financial support by the Deutsche Forschungsgemeinschaft, grants DE 1209/1-1 and STE 762/7-1.

Edited by
Weierstraß-Institut für Angewandte Analysis und Stochastik (WIAS)
Mohrenstraße 39
10117 Berlin
Germany

Fax: + 49 30 2044975
E-Mail: preprint@wias-berlin.de
World Wide Web: http://www.wias-berlin.de/

Abstract

Highly nonlinear wave propagation scenarios hold the potential to serve for energy concentration or pulse duration reduction of the input wave form, provided that a small range of input parameters be maintained. In particular when phenomena like rogue-wave formation or few-cycle optical pulses generation come into play, it becomes increasingly difficult to maintain control of the waveforms. Here we suggest an alternative approach towards the control of waveforms in a highly nonlinear system. Cascading pulse self-compression cycles at reduced nonlinearity limits the increase of input parameter sensitivity while still enabling an enhanced compression effect. This cascaded method is illustrated by experiments and in numerical simulations of the Nonlinear Schrödinger equation, simulating the propagation of short optical pulses in a self-generated plasma.

The occurrence of modulational instabilities or similar temporal pulse break-up scenarios is a characteristic feature of the nonlinear propagation of waves. Two prototypical examples for such events are the Benjamin-Feir instability [1] of deep-water waves and the azimuthal modulational instability of spatial solitons of the Nonlinear Schrödinger equation in optics [2]. Similar phenomena have been reported to occur in Bose-Einstein condensates [3], in plasma physics [4, 5], and in the propagation of short laser pulses [6, 7, 8, 9]. In self-generated optical filaments, temporal break-ups serve to actively compress femtosecond laser pulses [10, 11]. Recently, there has been revived interest in such phenomena as they can give rise to an unusual increase of pulse amplitude or concentration of energy and to the appearance of so-called rogue waves [12, 13]. The probability for the appearance of these rare events rapidly decreases with their amplitude. As the physical systems are deterministic, perfect control of the input wave should, in principle, enable an arbitrary increase of wave amplitude within the system's limitations. However, exploitation of rogue wave phenomena [14] is technically limited by the feasibility of control over the input wave. In most systems, a fundamental limitation also arises due to quantum noise [8]. In the following, we will present a new approach for exploiting rare events in a highly nonlinear system, cascading the process while at the same time limiting the underlying nonlinearity in every step. The latter measure maintains control over the output wave when exploiting such events, e.g., for waveform compression. We illustrate this cascaded waveform control for the propagation of short pulses in self-generated filament that are suitably described by the Nonlinear Schrödinger equation [10, 11]. In this system, pulse compression factors on the order of 3 to 5 have been previously discussed [15, 16, 17, 18, 19] in single-compression cycles. For an investigation of the double self-compression mechanism in noble gases, we perform numerical simulations of the generalized Nonlinear Schrödinger equation [18] which couples the envelope $\mathcal{E}$ of the electric field to the plasma density ρ of the medium according to

$$
\begin{aligned}
\partial_z \mathcal{E} &= \frac{i}{2k_0} T^{-1} \Delta_\perp \mathcal{E} + i\mathcal{D}\mathcal{E} + i\frac{\omega_0}{c} n_2 T |\mathcal{E}|^2 \mathcal{E} - i\frac{k_0}{2\rho_c} T^{-1} \rho(\mathcal{E})\mathcal{E} \qquad (1)\\
&- \frac{\sigma}{2}\rho\mathcal{E} - \frac{U_i W(I)(\rho_{nt}-\rho)}{2I}\mathcal{E}, \\
\partial_t \rho &= W(I)(\rho_{nt}-\rho) + \frac{\sigma}{U_i}\rho I \qquad (2)
\end{aligned}
$$

Here, $I = |\mathcal{E}|^2$ is the cycle-averaged field intensity. Assuming cylindrical symmetry, the transverse Laplacian may be reduced to $\Delta_\perp = (1/r)\partial_r r \partial_r$, where $r = (x^2+y^2)^{1/2}$ in cylindrical coordinates. Space-time focusing and self-steepening are introduced by the operator $T = 1 + \frac{i}{\omega_0}\partial_t$, the operator T^{-1} being evaluated in the Fourier domain. Correspondingly, the operator $\mathcal{D}$ modeling dispersion is treated in the Fourier domain according to

$$\tilde{\mathcal{D}}(\omega) = k(\omega) - k_0 - (\omega - \omega_0)\frac{\partial_k}{\partial_\omega}|_{\omega=\omega_0} \qquad (3)$$

where $k(\omega) = n(\omega)\omega/c$ is the wavenumber at the angular frequency ω, and $n(\omega)$ is the frequency dependent refractive index according to Ref. [20]. The carrier frequency of the laser field and corresponding wavenumber are denoted by ω_0 and k_0, respectively, with a carrier wavelength $\lambda = 800\,\mathrm{nm}$. n_2 is the nonlinear refractive index [21] and U_i corresponds to the ionization potential of the medium. Further on, $\rho_c = 1.73 \times 10^{21}\,\mathrm{cm}^{-3}$ is the critical plasma density at ω_0, and ρ_{nt} denotes the neutral density of the medium. σ is the cross section for collisional ionization. The ionization rate $W(I)$ is modelled according to Peremolov, Popov and Terent'ev [22] and adequately describes both multiphoton and tunneling ionization processes. The optical field envelope $\mathcal{E}$ is discretized on a numerical grid consisting of 6144×4096 points and propagated according to the generalized Nonlinear Schrödinger Equation (1). We use a parallelized algorithm on our HP Blade cluster consisting of 48 compute nodes, each being equipped with two Intel Xeon Quad-Core (X5355) CPUs. Based on experimental parameters discussed below, as initial conditions we assume 2.5 mJ optical input pulses at 800 nm and with initial beam waist $w_0 = 2.5\,\mathrm{mm}$ and pulse duration $t_{\mathrm{FWHM}} = 120\,\mathrm{fs}$, being focused by an $f = 1.5\,\mathrm{m}$ lens into a noble gas. To identify the small parameter range giving rise to compressed output waveforms on the axis of the filament, a parameter scan is performed by varying the gas pressure in a range from 100 to 120 kPa, at otherwise fixed input parameters, see Fig. 1. At a pressure $p = 106\,\mathrm{kPa}$, our simulations predict plasma-dominated dynamics in a relatively short nonlinear focal zone succeeded by a 1 m long self-generated channel, in which Kerr self-focusing effectively balances linear diffraction, see Fig. 1(a). This figure clearly reveals how a splitting event at $z = 1.4\,\mathrm{m}$ close to the linear focus position merges into formation of one isolated and shorter pulse. The splitting initially produces two pulses, one at $t = -100\,\mathrm{fs}$ and a second one at $t = +60$ fs. At $z = 1.6\,\mathrm{m}$, each of these subpulses is roughly 40 fs wide, which is a natural

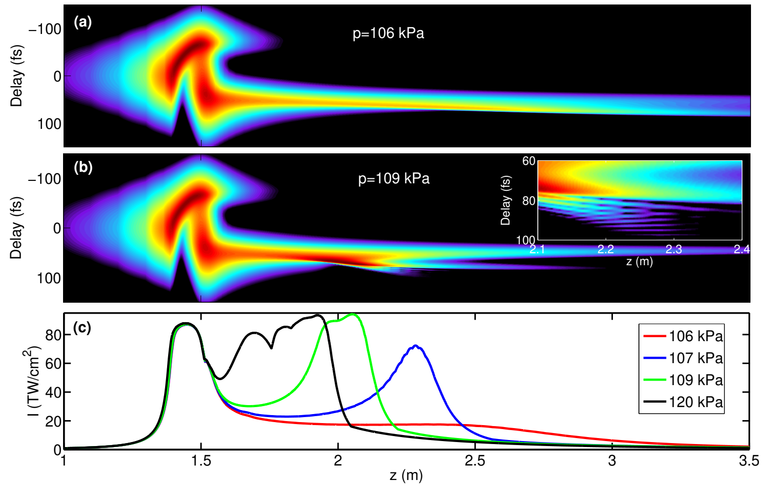

Figure 1: (a) Evolution of on-axis intensity profile along z for pulse self-compression into a sub-diffractive channel in argon, $p = 106\,\mathrm{kPa}$. (b) Corresponding evolution for the double self-compression scenario at $p = 109\,\mathrm{kPa}$. Inset: close-up on the pulse break-up in the second focus, accompanied by shock wave formation. (c) Evolution of on-axis peak intensity for pressure from 106 to 120 kPa.

consequence of the split. Upon further propagation ($z = 1.7\,\mathrm{m}$), the pulse at negative delays dies out quickly, leaving only one isolated and shortened pulse behind. This prototypical split-isolation cycle has already been discussed in [18, 19, 23] as the origin of on-axis pulse self-compression [17]. After the split-isolation cycle, plasma generation has effectively ceased, such that pulse shaping in the elongated channel at $z > 1.7\,\mathrm{m}$ is now dominated by an interplay between Kerr-type self-refraction and linear optical effects. Notably, self-focusing compensates diffractive optical effects, giving rise to a sub-diffractive nature of this final nonlinear propagation stage as also observed by Faccio *et al.* [24].

Increasing the pressure to $109\,\mathrm{kPa}$, we disturb the delicate balance in the non-diffractive channel by a slight increase of Kerr nonlinearity. This increase triggers a refocusing event $0.5\,\mathrm{m}$ behind the first nonlinear focus, and a second strongly ionized zone evolves [Figs. 1(b),(c)]. Here the pulse experiences a second split-isolation cycle that shows superficially the same behavior as the first one, i.e., the surviving pulse from the first cycle splits into two at $z = 2.2\,\mathrm{m}$. In contrast to the first cycle, the trailing pulse dies out at $t \approx 80\,\mathrm{fs}$, leaving only one isolated and yet again shortened pulse at $t \approx 50\,\mathrm{fs}$ behind. In the subsequent nonlinear propagation inside the channel, the pulse reaches a minimum duration of $16.4\,\mathrm{fs}$ at $z = 2.5\,\mathrm{m}$. Further increasing the pressure to $p = 120\,\mathrm{kPa}$, pulses with a minimum duration of $10.9\,\mathrm{fs}$ emerge after the second focus. This nearly twelvefold compression chiefly goes back to the two split-isolation cycles. Such a strong compression effect has neither been observed in previous experimental[17, 15, 16] nor theoretical studies[18, 19]. The emergence of the refocusing event must not be confused with focusing-defocusing cycles [25] that occur on significantly shorter length scales of $\approx 20\,\mathrm{cm}$ whereas repetition of the split-isolation cycle is only observed with a distance $> 50\,\mathrm{cm}$ between the events. Also focusing-defocusing cycles have been discussed to provide a less drastic effect on the pulse shape.

Despite the apparently identical effect on pulse duration, collapse saturation in the two foci is accomplished by different physical effects. In the first nonlinear focus ($z = 1.5\,\mathrm{m}$), plasma defocusing and related dissipative terms clamp the intensity whereas temporal effects, in particular dispersion, take over this role in the second focus ($z = 2\,\mathrm{m}$). Indeed, neglecting the plasma response for $z > 1.75\,\mathrm{m}$ in the simulation at $p = 107\,\mathrm{kPa}$ [Fig. 1(c), blue line] leads to a nearly unchanged dynamical behavior for the second compression stage. Similar plasmaless refocusing events have been discussed in Refs. [26, 27]. With increasing pressure ($p \geq 1.09\,\mathrm{bar}$), however, plasma becomes again essential for preventing spatial wave collapse, while dispersion dominates temporal dynamics by exchanging power between different pulse time slices. The generation of dispersive shock waves in the trailing edge of the pulse [Fig. 1(b), inset] during the second splitting event further underlines the strong impact of dispersion and self-steepening.

We have investigated experimental prerequisites for observation of the cascaded scenario and found that a more than tenfold total compression factor strongly relies on the availability of optical pulses with several millijoule energy and 120 fs pulse duration. We find that these conditions are currently difficult to meet with available laser sources, which is more a consequence of the rather long pulse duration than that of a narrowed input parameter range (see discussion below). We therefore looked for other evidence of the pulse shaping action in the second focus. For this purpose, we computed XFROG spectrograms from the simulated on-axis data, see Fig. 2. In the single self-compression regime, these representations exhibit a characteristic shape that are most suitably described as the mirror image of the Greek letter Γ [Fig. 2(a)], as has already been discussed in [18]. A short pulse duration is intimately connected to a vanishing slant of the vertical bar of the Γ. The extension of this section towards the blue is a measure of the asymmetric nonlinear spectral broadening effects, mainly caused by self-steepening [28]. The appearance of pronounced horizontal structures along the cap section of the Γ, in contrast, is connected to the suppression of the leading pulse in the split-isolation cycle, i.e., pulse contrast. If a second split-isolation cycle appears, the spectro-temporal pattern of the pulses changes in a characteristic way, see Fig. 2(b). Remnants of the suppressed pulse after the second split-isolation cycle now appear as a blue trailing pedestal of the spectrogram, i.e., point symmetric to the red leading pedestal appearing after the first cycle, with a shape that we will refer to as Q-shape in the following. The broadening effect appears as a spectral red-shift along the vertical axis in Fig. 2(b).

Figure 3(a) shows a more detailed view of the transition from inverse Γ to Q-shape, with a zoomed-in set of spectrograms computed in the range from $z = 195$ to $245\,\mathrm{cm}$. In the initial spectrograms in this sequence, the typical Γ shape appears with the

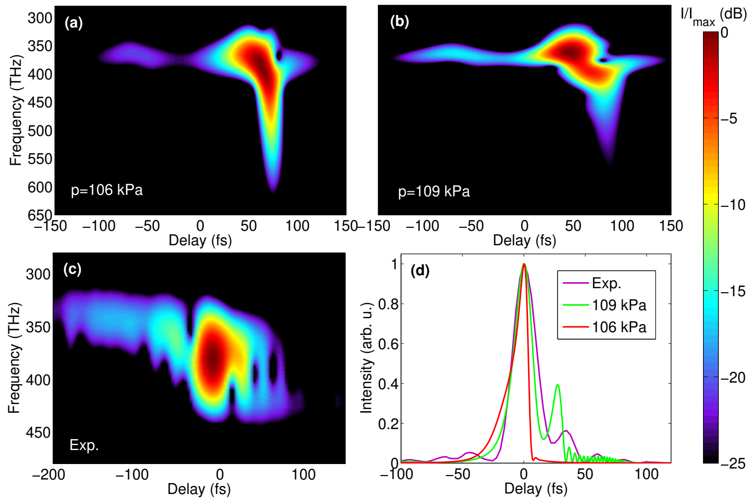

Figure 2: On-axis XFROG spectrograms (a) of the optical field emerging from the sub-diffractive channel regime of Fig 1(a), $z = 2.5\,\mathrm{m}$, $p = 106\,\mathrm{kPa}$ and (b) after the second pulse breaking at $z = 2.45\,\mathrm{m}$, $p = 109\,\mathrm{kPa}$, two-foci regime. (c) XFROG spectrogram retrieved from experimental SPIDER interferogram in air after double self-compression. (d) Corresponding on-axis temporal intensity profiles.

vertical bar extending into the blue spectral range. During the approach towards the second focus, however, the spectral extension into the blue reduces, with a red-shift appearing shortly afterward. Emergence of the red-shift comes along with formation of a blue pedestal, which is ultimately a remnant of the blue wing of the inverse Γ shape. Figure 3(b) additionally shows a view of angularly resolved spectra [24] during this transition phase. These structures exhibit a markedly different behavior in the blue and the red wing of the pulse. This behavior is related to the strong influence of self-steepening, which causes the blueshift in the trailing part of the pulse. In fact, the modulational instability occurring in self-focusing media with normal group velocity dispersion reshapes this part of the pulse into a characteristic X-shaped spatio-spectral pattern [29]. In the spatio-temporal domain, this instability has also been shown to be responsible for the observed temporal splitting and the emergence of hyperbolic shock waves [30, 31]. Remarkably, those dispersion dominated dynamics are still observable in the pressure regime above 109 kPa, where plasma defocusing is already essential for wave-collapse arrest. The apparent red-shift of the spectra of the optical fields emerging from the 2-foci regime can thus be ascribed to both, self-phase modulation in the leading edge of the pulse during the refocusing stage and to angular dispersion of the blue spectral content of the pulse into a spatial reservoir due to the generation of the shock wave.

For experimental verification of the double self-compression, we employed a 45 fs regenerative Ti:sapphire amplifier system with a pulse energy of 5 mJ to produce femtosecond filaments in air. The laser pulse energy has been carefully attenuated by means of an adjustable diaphragm until a single filament with two clearly sepa-

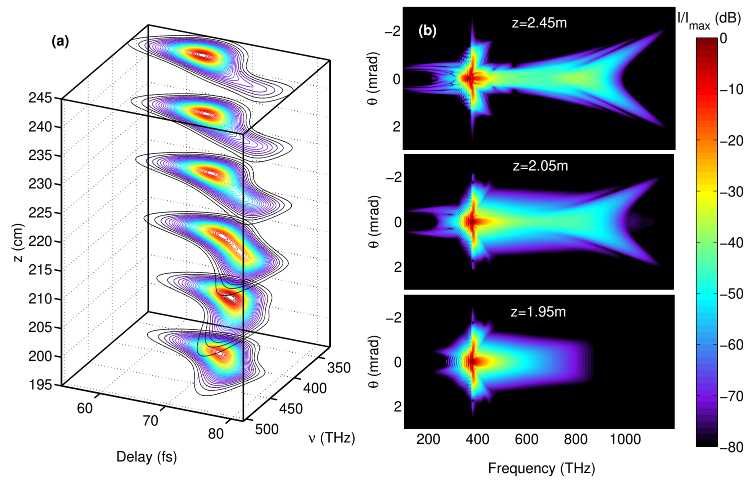

Figure 3: (a) Evolution of XFROG spectogram along z during propagation through the second focus. (b) Corresponding angularly resolved far-field spectra.

rated strongly ionized zones appeared that were separated by about 30-40 cm. With these short input pulses, our simulations indicate that we can at best expect fourfold compression. For a check on the spectro-temporal structure of the pulses, the filament output has been characterized with the SPIDER method [32] in amplitude and phase, see Fig. 2(d). For comparison, we computed XFROG spectrograms from the data, see Fig. 2(c). This spectrogram shows features previously discussed for the single-focus and the double-focus regime, cf. Fig. 2(a) and (b), respectively. From the former, a temporally stretched leading pedestal is discernible, which is generally quite typical for self-compression [18]. In addition to previous experimental findings, however, a clearly visible trailing blue pedestal appears. To the best of our knowledge, such a structure has not been reported in literature yet. It is striking that this feature appears temporally less stretched than the leading red pedestal from the first split-isolation cycle, which corroborates less exposure to linear and nonlinear pulse shaping effects. Therefore the experimental findings appear to be highly compatible with the causal sequence of events predicted by numerical simulation. This finding also suggests that the second split-isolation cycle is being caused by a different mechanism as the first one, causing pedestal formation at opposing spectral and temporal edges of the main pulse.

The cascaded compression scenario is not an isolated phenomenon, but can be obtained for a range of input pulse parameters and gas species, which sets it apart from a highly optimized single-compression scenario. Assuming krypton as the nonlinear medium [20, 21], for a demonstration of the universality of this mechanism we have scanned the parameter range of input pulse energy and peak power in numerical simulations for appearance of this phenomenon. Beam waist and temporal duration were fixed at $w_0 = 5\,\mathrm{mm}$ and $t_{\mathrm{FWHM}} = 120\,\mathrm{fs}$, respectively. The observed pulse shortening as a function of input energy and system nonlinearity (peak power

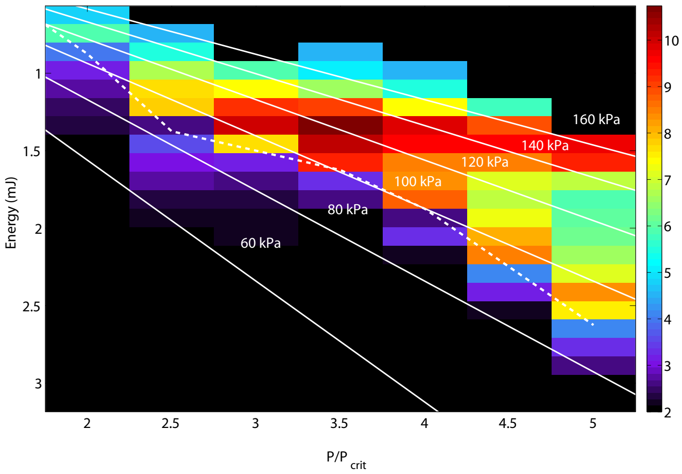

Figure 4: Pulse compression ratio in a krypton filament for various initial conditions in the Energy vs $P/P_{\rm cr}$ plane. The solid lines correspond to lines of equal pressure. The dashed line seperates subdiffrative channel regimes (below) from double self-compression regimes (above).

normalized to $P_{\rm cr}$) is depicted in Fig. 4, with iso-pressure lines shown in white. The dashed line, roughly collinear with the 100 kPa pressure line, marks the lower limit of double self-compression. From this picture, the capability of the cascaded self-compression becomes immediately clear, giving rise to up to twelvefold compression. Compression ratios above 10 are localized in the region of double self-compression and can already be observed at powers exceeding the critical power by a factor of only three. Our scan also reveals examples for threefold cascading of the split-isolation cycle, yet with imperfect isolation in the last cycle. Generally, for pressures exceeding 160 kPa we observe an increased tendency for such undesired multiple temporal splits. Importantly, cascaded self-compression fills a considerable fraction of the parameter space mapped out in Fig. 4. This sets it apart from sparsely represented rogue-wave-like events [13].

Our numerical investigations and experimental studies pinpoint an alternative approach toward efficient exploitation and control of highly nonlinear wave shaping mechanisms. Rather than trying to confine input parameters in an increasingly narrow range, it appears much more promising to relax these constraints in order to avoid that input noise strongly affects the output waveform. We demonstrated that physical systems exist that allow for cascaded application of the waveform shaping effect, e.g., in order to compress optical pulses or to concentrate energy. While this effect certainly also narrows the input parameter space, this effect is minor as compared to immediate rogue wave control that exhibits a rapidly imploding parameter space with increasing amplitude [12]. Our cascaded compression method therefore opens a perspective not only for optical pulse compression but for exploitation of waveform control in a wide range of similar highly nonlinear physical scenarios.

We thank Erik T.J. Nibbering and Thomas Elsaesser, Max-Born-Institut, Berlin, for helpful discussions. Financial support by the Deutsche Forschungsgemeinschaft, grants DE 1209/1-2 and STE 762/7-2, is gratefully acknowledged.

References

[1] T. B. Benjamin and J. E. Feir, J. Fluid Mech. **27**, 417-430 (1967).

[2] V. I. Bespalov and V. I. Talanov, JETP Lett. **11**, 471 (1966).

[3] A. Smerzi, A. Trombettoni, P. G. Kevrekidis, and A. R. Bishop, Phys. Rev. Lett. **89** 170402 (2002).

[4] S. Champeaux, T. Passot, and P. L. Sulem, J. Plasma Phys. **58**, 665–690 (1997)

[5] E. Mjolhus, J. Plasma Phys. **16**, 321 (1976).

[6] K. Tai, A. Hasegawa, A. Tomita, Phys. Rev. Lett. **56**, 135–138 (1986).

[7] S. M. J. Kelly, Electron. Lett. **28**, 806–807 (1992).

[8] J. M. Dudley, G. Genty, F. Dias, B. Kibler, and N. Akhmediev, Opt. Express **17**, 21497–21508 (2009).

[9] A. Demircan and U. Bandelow, Appl. Phys. B **86**, 31 (2007).

[10] A. Couairon and A. Mysyrowicz, Phys. Rep. **441**, 47–189 (2007).

[11] L Bergé, S. Skupin, R. Nuter, J. Kasparian, and J.-P. Wolf, Rep. Prog. Phys. **70**, 1633-1713 (2007)

[12] D. R. Solli, C. Ropers, P. Koonath, and B. Jalali, Nature **450**, 1054 (2007).

[13] J. Kasparian, P. Bejot, J. P. Wolf, J. M. Dudley, Opt. Express **17** 12070–12075 (2009).

[14] D. R. Solli, C. Ropers, and B. Jalali, Phys. Rev. Lett. **101**, 233902 (2008).

[15] O. G. Kosareva *et al.*, Appl. Phys. B **91**, 35–43 (2008).

[16] C. P. Hauri *et al.*, Opt. Lett. **32**, 868–870 (2007)

[17] G. Stibenz, N. Zhavoronkov, and G. Steinmeyer, Opt. Lett. **31**, 274 (2006).

[18] S. Skupin *et al.*, Phys. Rev. E **74**, 056604 (2006).

[19] C. Brée, A. Demircan, S. Skupin, L. Bergé, and G. Steinmeyer, Opt. Express. **17**, 16429 (2009).

[20] A. Dalgarno and A. E. Kingston, Proc. Roy. Soc. A **259**, 424 (1960).

[21] H. J. Lehmeier, W. Leupacher, and A. Penzkofer, Opt. Commun., **56**, 67 (1985).

[22] A. M. Peremolov, V. S. Popov, M. V. Terent'ev, Sov. Phys. JETP **23**, 924 (1966)

[23] C. Brée, A. Demircan, S. Skupin, L. Bergé, and G. Steinmeyer, to appear in Laser Phys.

[24] D. Faccio, A. Averchi, A. Lotti, P. Di Trapani, A. Couairon, D. Papazoglou, and S. Tzortzakis, Opt. Express **16**, 1565–1570 (2008).

[25] L. T. Vuong, R. B. Lopez-Martens, C. P. Hauri, and A. L. Gaeta, Opt. Express **16**, 390–401 (2008).

[26] S. Champeaux and L. Bergé, Phys. Rev. E **71**, 046604 (2005).

[27] S. Eisenmann, A. Pukhov, and A. Zigler, Phys. Rev. Lett. **98**, 155002 (2007).

[28] A. L. Gaeta, Phys. Rev. Lett. **84**, 3582 (2000).

[29] M. A. Porras, A. Parola, D. Faccio, A. Couairon, and P. Di Trapani, Phys. Rev. A **76**, 011803(R) (2007).

[30] L. Bergé *et al.*, J. Opt. Soc. Am. B **13**, 1879 (1996).

[31] L. Bergé, K. Germaschewski, R. Grauer, and J. J. Rasmussen, Phys. Rev. Lett. **89**, 153902 (2002).

[32] G. Stibenz and G. Steinmeyer, Rev. Sci. Instrum. **77**, 073105 (2006).